

## ORIGINAL ARTICLE

# Trans-repression of NF $\kappa$ B pathway mediated by PPAR $\gamma$ improves vascular endothelium insulin resistance

Ying Kong<sup>1,2</sup> | Yan Gao<sup>1,2</sup> | Dongyi Lan<sup>3</sup> | Ying Zhang<sup>1,2</sup> | Rixin Zhan<sup>1,2</sup> |  
Meiqi Liu<sup>1,2</sup> | Zhouan Zhu<sup>3</sup> | Guohua Zeng<sup>1,2</sup> | Qiren Huang<sup>1,2</sup> 

<sup>1</sup>Key Provincial Laboratory of Basic Pharmacology, Nanchang University, Nanchang, Jiangxi, China

<sup>2</sup>Department of Pharmacology, School of Pharmacy, Nanchang University, Nanchang, Jiangxi, China

<sup>3</sup>Jiangxi Medical College, Nanchang University, Nanchang, Jiangxi, China

## Correspondence

Qiren Huang, Key Provincial Laboratory of Basic Pharmacology, Nanchang University, Nanchang, Jiangxi, China.  
Email: qrhuang@ncu.edu.cn

## Funding information

The National Natural Scientific Foundation of China, Grant/Award Number: 81070633, 81360060, 31660323, 30860111; The Jiangxi Provincial Department of Science & Technology, Grant/Award Number: 20123BCB22005

## Abstract

Previous study has shown that thiazolidinediones (TZDs) improved endothelium insulin resistance (IR) induced by high glucose concentration (HG)/hyperglycaemia through a PPAR $\gamma$ -dependent-NF $\kappa$ B trans-repression mechanism. However, it is unclear, whether changes in PPAR $\gamma$  expression affect the endothelium IR and what the underlying mechanism is. In the present study, we aimed to address this issue. HG-treated human umbilical vascular endothelial cells (HUVEC) were transfected by either PPAR $\gamma$ -overexpressing (Ad-PPAR $\gamma$ ) or PPAR $\gamma$ -shRNA-containing (Ad-PPAR $\gamma$ -shRNA) adenoviral vectors. Likewise, the rats fed by high-fat diet (HFD) were infected by intravenous administration of Ad-PPAR $\gamma$  or Ad-PPAR $\gamma$ -shRNA. The levels of nitric oxide (NO), endothelin-1 (ET-1) and cytokines (TNF $\alpha$ , IL-6, sICAM-1 and sVCAM-1) and the expression levels of PPAR $\gamma$ , eNOS, AKT, p-AKT, IKK $\alpha/\beta$  and p-IKK $\alpha/\beta$  and I $\kappa$ B $\alpha$  were examined; and the interaction between PPAR $\gamma$  and NF $\kappa$ B-P65 as well as vascular function were evaluated. Our present results showed that overexpression of PPAR $\gamma$  notably increased the levels of NO, eNOS, p-AKT and I $\kappa$ B $\alpha$  as well as the interaction of PPAR $\gamma$  and NF $\kappa$ B-P65, and decreased the levels of ET-1, p-IKK $\alpha/\beta$ , TNF $\alpha$ , IL-6, sICAM-1 and sVCAM-1. In contrast, down-expression of PPAR $\gamma$  displayed the opposite effects. The results demonstrate that the overexpression of PPAR $\gamma$  improves while the down-expression worsens the endothelium IR via a PPAR $\gamma$ -mediated NF $\kappa$ B trans-repression dependent manner. The findings suggest PPAR $\gamma$  is a potential therapeutic target for diabetic vascular complications.

## KEYWORDS

endothelium, inflammation, insulin resistance, NF $\kappa$ B, PPAR $\gamma$

## 1 | INTRODUCTION

Insulin resistance (IR) refers to a decrease in sensitivity to insulin for insulin target tissues including muscle, liver and adipose tissue, etc

and is well-characterized as an independent risk factor for the development of type 2 diabetes mellitus (T2DM) and atherosclerosis (AS).<sup>1-3</sup> Moreover, IR is also associated with a wide range of traditional and non-traditional risk factors for cardiovascular diseases (eg endothelial dysfunction, dyslipidemia, inflammation, vascular wall abnormalities).<sup>4</sup> Previously, insulin actions on muscle, liver and adipose tissue have been fully described.<sup>5-7</sup> However, the role of IR in

Ying Kong, Yan Gao, and Dongyi Lan are the authors who contributed equally to this article.

This is an open access article under the terms of the Creative Commons Attribution License, which permits use, distribution and reproduction in any medium, provided the original work is properly cited.

© 2018 The Authors. Journal of Cellular and Molecular Medicine published by John Wiley & Sons Ltd and Foundation for Cellular and Molecular Medicine.

non-canonical tissues, such as the endothelium, is less clear. Several studies support a role for IR in the development of premature cardiovascular AS independent of T2DM and obesity,<sup>8,9</sup> but the cause of IR is still poorly understood.

Peroxisome proliferator-activated receptor  $\gamma$  (PPAR $\gamma$ ), a super-family member of nuclear transcription factors, plays essential roles in gluco-lipid homeostasis and adipogenesis and it is a molecular target of insulin-sensitizing drugs such as thiazolidinediones (TZDs).<sup>10</sup> As exogenous agonists of PPAR $\gamma$ , TZDs affect multiple pathophysiological processes such as lipid metabolism, vascular modifications and production of inflammatory mediators, which are involved in the development of diabetic cardiovascular complications.<sup>11-13</sup> For example, TZDs decrease plasminogen activator-1 and C-reactive protein levels<sup>14</sup> as well as reduce coronary hyperplasia after coronary stent implantation.<sup>15</sup> Insulin-sensitizing therapy with TZDs is considered as a promising intervention for patients with T2DM.<sup>16</sup> However, numerous clinical studies have shown that TZDs have many side effects including fluid retention, worsening heart failure and weight gain.<sup>17</sup> Therefore, reduction in side effects of TZDs especially negative effects on cardiovascular system is needed.

Although TZDs have anti-diabetic and anti-atherogenic effects by acting on macrophages and lymphocytes by trans-repressing nuclear factor kappaB- (NF $\kappa$ B-) dependent target genes,<sup>18</sup> the effects of TZDs on vascular endothelial cells and the underlying mechanisms remain poorly understood. Our recent data revealed that TZDs improved vascular endothelium IR induced by high concentration of glucose /hyperglycaemia (HG) through a PPAR $\gamma$ -dependent NF $\kappa$ B trans-repression mechanism.<sup>19</sup> However, it is unclear whether changes in PPAR $\gamma$  expression affect endothelium IR and what the underlying mechanism is. Therefore, in the present study, we sought to investigate the effects of alterations of PPAR $\gamma$  expression on endothelium IR and explore its underlying molecular mechanisms.

## 2 | MATERIALS AND METHODS

### 2.1 | Reagents

Dulbecco's modified Eagle's medium (DMEM) and foetal bovine serum (FBS) were purchased from Gibco-BRL (NY, USA). The assay kits for tumour necrosis factor alpha (TNF $\alpha$ ), interleukin-6 (IL-6), soluble intercellular adhesion molecule-1 (sICAM-1), soluble vascular cellular adhesion molecule-1 (sVCAM-1) and endothelin-1 (ET-1) were bought from R&D Systems, Inc. (MN, USA), and NO assay kit from Beyotime Institute of Biotech (Shanghai, CHN). Streptozotocin (STZ), acetylcholine (Ach), sodium nitroprusside (SNP), phenylephrine (PE) and dimethyl sulfoxide (DMSO) and all other chemicals were commercially obtained from Sigma-Aldrich (St. Louis, MO, USA) unless indicated elsewhere. Antibodies against PPAR $\gamma$ , endothelial nitric oxide synthase (eNOS), AKT and phosphor-AKT (p-AKT), inhibitory  $\kappa$ B kinase alpha/beta (IKK $\alpha/\beta$ ) and phosphorylated-inhibitory  $\kappa$ B kinase alpha/beta (p-IKK $\alpha/\beta$ ) and inhibitory  $\kappa$ B alpha (I $\kappa$ B $\alpha$ ) were purchased from Cell Signaling Technology, Inc. (MA, USA), and antibody against  $\beta$ -actin from Santa Cruz (CA, USA).

### 2.2 | Cell lines and adenoviral vectors

The human umbilical vascular endothelial cells (HUVEC, Catalog No: CRL-1730), 3T3-L1 (Catalog No: CL-173) and HEK293T (Catalog No: CRL-3216) cells were all obtained from the American Type Culture Collection (ATCC, US). PPAR $\gamma$ -overexpressing adenoviral vector (Ad-PPAR $\gamma$ ) and PPAR $\gamma$ -short hair RND (shRNA)- containing adenoviral vector (Ad-PPAR $\gamma$ -shRNA) were purchased from Genechem. Tech. Inc. (Shanghai, CHN).

### 2.3 | Cell culture

Cultures of HUVEC and HEK293T were performed as described in our previous study.<sup>20</sup> Briefly, the cells were cultured in gelatin-coated six-well plates and propagated in DMEM, which was supplemented with 10% FBS, 100 IU mL<sup>-1</sup> penicillin and 0.1 mg mL<sup>-1</sup> streptomycin. The cells were cultured at 37°C in a 95% O<sub>2</sub>-5% CO<sub>2</sub> humidified atmosphere.

The culture and differentiation of the 3T3-L1 cells were carried out as previously described in our study.<sup>21</sup> Briefly, 60% confluent 3T3-L1 cells were incubated in the serum-free DMEM/F12 medium supplemented with an adipogenic cocktail which contains 1 m mol L<sup>-1</sup> dexamethasone, 66 n mol L<sup>-1</sup> insulin, 15 m mol L<sup>-1</sup> HEPES, 1 n mol L<sup>-1</sup> T3, 33 m mol L<sup>-1</sup> biotin, 17 m mol L<sup>-1</sup> pantothenate, 10 mg mL<sup>-1</sup> transferrin, 100 mg mL<sup>-1</sup> penicillin-streptomycin and 1 mg mL<sup>-1</sup> rosiglitazone for 8 days. During the differentiation, the medium was replaced every 2 days.

### 2.4 | Establishment of endothelium IR model in vitro and in vivo

The methods for establishment of endothelium IR model in vitro and in vivo have previously been described in details.<sup>19</sup> Briefly, HUVEC with a 90% confluence was first pre-treated with a complete DMEM containing 33 m mol L<sup>-1</sup> of glucose (HG) for 48 hours. After that, the DMEM was replaced by a fresh serum-free medium and then the HUVEC was further cultured for 4 hours. Subsequently, the cells were treated with 5 mIU L<sup>-1</sup> insulin (final concentration) for 10 minutes. Finally, the supernatants were collected and the levels of nitrite and ET-1 were assayed; and the cells were used to detect the expression of AKT and p-AKT.

All animal procedures were approved by the Institutional Animal Care and Use Committee of Nanchang University School of Medicine and conducted in accordance with the guide for the Care and Use of Laboratory Animals published by the US National Institute of Health (NIH Publication No.85-23, revised 1996). Briefly, male Sprague-Dawley (SD) rats weighing 150-180 g (provided by Department of Experimental Animals, Nanchang University, CHN) were fed with standard chows and water *ad libitum*, prior to the dietary manipulation. The rats were randomly allocated into two dietary regimens by feeding with either standard chows (Control, 10 rats) or high-fat diet (HFD, 58% fat, 25% protein and 17% carbohydrate in the proportion of total kcal, 30 rats) *ad libitum* respectively, for a period of 6 weeks.

At the end of 2 weeks after dietary manipulation, the HFD-fed rats were injected intraperitoneally (i.p.) with a low dose of STZ (35 mg kg<sup>-1</sup>) while the control rats were given the vehicle for STZ (ie citrate buffer, pH 4.4, 1 mL kg<sup>-1</sup>, i.p.) respectively. Physical parameters including body weight, body length, body mass index (BMI) and fat coefficient were measured. Also, fasting plasma glucose (FPG) and serum insulin (FINS), triglyceride (TG), cholesterol (CH) as well as the homeostatic model assay of IR (HOMA-IR) were tested. In addition, the serum levels of nitrite and ET-1 as well as the expression of AKT and p-AKT from aorta tissue were assayed before modelling (pre-model) and after modelling (post-model).<sup>19</sup>

## 2.5 | Expression levels of PPAR $\gamma$ in HEK293T and 3T3-L1 cells with post-transfection of different adenoviral vectors

The 90% confluent HEK293T cells were transfected with adenoviruses containing either wild-type full-length cDNA of PPAR $\gamma$  (PPAR $\gamma$ ) or a cDNA-scramble of PPAR $\gamma$  (vehicle, Veh). Similarly, 3T3-L1 cells were transfected with adenoviruses containing either a shRNA of PPAR $\gamma$  (shRNA) or a shRNA-scramble of PPAR $\gamma$  (vehicle, Veh). The cells that were not transfected were considered as the normal control (Ctrl). After transfection for 24 hours, fresh complete DMEM was added and these cells were further cultured for another 12 hours. Finally, the cells were harvested and PPAR $\gamma$  expression levels were detected by Western blots.

## 2.6 | In vitro experimental protocols

The 90% confluent HUVEC was first pre-treated with a fresh complete DMEM containing HG for 48 hours and then further cultured for 4 hours with a fresh serum-free DMEM (IR). Next, the cells were randomly allocated to two batches. One batch of cells was transfected with adenoviruses containing either wild-type full-length cDNA of PPAR $\gamma$  (IR+PPAR $\gamma$ ) or a cDNA-scramble of PPAR $\gamma$  (vehicle, IR+Veh); while the other was done with those containing either a shRNA of PPAR $\gamma$  (IR+shRNA) or a shRNA-scramble of PPAR $\gamma$  (vehicle, IR+Veh). The cells that were neither treated with HG nor transfected were considered as the Ctrl. After transfection for 24 hours, all the cells were washed with PBS twice and further cultured with the fresh serum-free DMEM for an additional 12 hours. At the end, the supernatants were used to test the levels of NO, ET-1 and cytokines (TNF $\alpha$ , IL-6, sICAM-1 and sVCAM-1) and the cells were used to measure the expression levels of PPAR $\gamma$ , eNOS, AKT, p-AKT, IKK $\alpha/\beta$ , p-IKK $\alpha/\beta$  and I $\kappa$ B $\alpha$ . Besides, the interaction between PPAR $\gamma$  and NF $\kappa$ B-P65 was evaluated by immunoprecipitation.

## 2.7 | In vivo experimental protocols

The rats with systemic and endothelium IR were first randomly divided into five groups (Six rats per group), ie IR, IR+Ad-PPAR $\gamma$  (IR+PPAR $\gamma$ ), IR+Ad-PPAR $\gamma$ -shRNA (IR+shRNA) and their respective scrambles (IR+Veh). The rats were intravenously administered with

Ad-PPAR $\gamma$  (IR+PPAR $\gamma$  group), Ad-PPAR $\gamma$ -shRNA (IR+shRNA), their vehicles (IR+Veh groups), normal saline (IR group). The six rats that were neither treated with HFD nor transfected were considered as the Ctrl group. After treatment for a week, serum levels of NO, ET-1 and other cytokines (TNF $\alpha$ , IL-6, sICAM-1 and sVCAM-1) were assayed, functional assessment of rat aorta was performed, and expression levels of PPAR $\gamma$ , eNOS, AKT, p-AKT, IKK $\alpha/\beta$ , p-IKK $\alpha/\beta$  and I $\kappa$ B $\alpha$  from aorta were determined by Western blots.

## 2.8 | Functional assessment of rat aorta

The functional assessment of rat aorta was carried out by a modification of the previously described method.<sup>22</sup> Briefly, all the rats were fasted for 12 hours and anaesthetized with ketamine (70 mg kg<sup>-1</sup>, ip). Then, the rats were sacrificed by a cervical dislocation. The thoracic aorta was carefully isolated and an approximately 3 mm long aortic ring for each of the rat was prepared. The ring was isometrically mounted on a myograph (model 610M, DMT, Denmark). The aortic ring was first equilibrated for 45 minutes under a resting tension of 0.5 g and then was pre-treated with 1  $\mu$  mol L<sup>-1</sup> PE. The concentration-response curves to acetylcholine (Ach, 10<sup>-10</sup>-10<sup>-5</sup> M) or sodium nitroprusside (SNP, 10<sup>-10</sup>-10<sup>-5</sup> M) were performed after 40%-60% maximal contraction was induced with 1  $\mu$  mol L<sup>-1</sup> PE (. The vasodilation at each concentration was measured and expressed as the percentage of force generated in response to PE.

## 2.9 | Western blots for protein expression levels

Western blots were performed according to the method described in our previous study with a minor modification.<sup>23</sup> Briefly, cells were washed with PBS twice, disrupted on ice for 30 minutes in NP-40 (50 n mol L<sup>-1</sup> Tris (pH 7.4), 1% NP-40, 150 m mol L<sup>-1</sup> NaCl and 40 m mol L<sup>-1</sup> NaF) or RIPA lysis buffer (Thermo Scientific, Shanghai, CHN) supplemented with the protease and phosphatase inhibitors (Pierce Chemical, Dallas, US) and cleared by centrifugation. Protein concentration was determined with a BCA protein quantification kit. Equal amount of protein (35  $\mu$ g) in cell lysates was first separated by SDS-PAGE, next transferred to polyvinylidene difluoride (PVDF) membranes followed by immunoblot with specific primary antibodies at a 1:1000 dilution and second antibodies at a 1:2000 dilution, and then detected by chemiluminescence with the ECL detection reagents (Amersham Biosciences, London, UK).  $\beta$ -actin was used as a loading control.

## 2.10 | Quantitative assay of ET-1 and cytokines by ELISA

Quantitative assay for ET-1 and cytokines (TNF $\alpha$ , IL-6, sICAM-1 and sVCAM-1) in the supernatants or in rat serum was performed using the Quantikine ELISA Kits according to the manufacturer's instruction. Briefly, 50  $\mu$ L serum or cell supernatant was added to a 96-well polystyrene microplate pre-coated with various monoclonal antibodies against the corresponding cytokines and incubated for 2 hours at

room temperature on the shaker. After five times of gentle washes with PBS, 100  $\mu$ L secondary antibodies conjugated to horseradish peroxidase were added and incubated for 2 hours at room temperature, followed by an addition of 100  $\mu$ L substrate solutions and incubation for 30 minutes at room temperature. Then, 100  $\mu$ L stop solution was added and the optical density (OD) was read at 450 nm in a microplate reader (Bio-Rad Laboratories, Hercules, USA).

### 2.11 | Measurement of nitrite

The levels of nitrite were determined by a nitrite assay kit according to the manufacturer's instruction. Since the NO is very unstable and rapidly converted into nitrite, nitrite concentrations were measured to indicate NO levels. Nitrite reacts with Griess reagents to produce a colour, which can be measured by a spectrophotometer at 550 nm. Briefly, a standard curve was prepared using a series of nitrite concentrations. 100  $\mu$ L of the sample was added into a 96-well microplate and then the Griess reagent I and II were in turn added and mixed. Next, the mixture was incubated at 37°C for 60 minutes. Finally, the OD was determined at 550 nm with a spectrophotometer (Bio-Rad Laboratories).

### 2.12 | Statistical analysis

All data were expressed as the mean  $\pm$  SEM. Significance was tested with unpaired *t* test, one-way ANOVA and homogeneity test of variance wherever appropriate. *P* value <0.05 was considered to be statistically significant.

## 3 | RESULTS

### 3.1 | PPAR $\gamma$ expression levels in HEK293T, 3T3-L1 and vascular endothelial cells in vitro and in vivo

To investigate the role of PPAR $\gamma$  in fine-tuning vascular endothelium IR induced by HG or HFD, over- and down-expressional adenoviral vectors targeting PPAR $\gamma$  gene were constructed. To test whether the vectors were successfully constructed, three cell lines including HEK293T, 3T3-L1 and HUVEC as well as rat aortic vascular endothelium were used to determine the PPAR $\gamma$  expression levels. As anticipated, HEK293T cells had constitutive expression levels, whereas 3T3-L1 cells had considerably abundant expression of PPAR $\gamma$ . Transfection of Ad-PPAR $\gamma$  into HEK293T increased the expression levels of PPAR $\gamma$  by 248% (vs. Veh or Ctrl, Figure 1A); while transfection of Ad-PPAR $\gamma$ -shRNA into 3T3-L1 decreased those by 29% (vs. Veh or Ctrl, Figure 1B). Moreover, constitutive PPAR $\gamma$  expression in the Ctrl (HUVEC in vitro and rat vascular endothelium in vivo) group was found, while that in IR or IR+Veh group decreased significantly compared with Ctrl group. However, due to transfection of the over- or down-expressional adenoviral vectors, the expression levels of PPAR $\gamma$  were notably up-regulated or down-regulated respectively (vs. IR+Veh, Figure 1C,F), indicating that the vectors were successfully constructed and the transfection met the experimental needs.

### 3.2 | Amelioration of vascular endothelium IR in vitro and in vivo by PPAR $\gamma$

The extent of endothelium IR was evaluated by the levels of NO and ET-1 stimulated by insulin.<sup>24</sup> As shown in Figure 2, HG or HFD markedly decreased the levels of NO and p-AKT but increased the levels of ET-1 both in vitro and in vivo (vs. Ctrl), indicating that the endothelium IR was elicited. Overexpression of PPAR $\gamma$  (ie IR+PPAR $\gamma$  group) normalized the decreased levels of NO and p-AKT and the increased levels of ET-1 induced by HG or HFD both in vitro and in vivo (vs. IR or IR+Veh group), demonstrating overexpression of PPAR $\gamma$  ameliorated considerably the endothelium IR induced by HG or HFD. However, down-expression of PPAR $\gamma$  (ie IR+shRNA group) exacerbated the changes in the levels of NO and p-AKT as well as ET-1 induced by HG or HFD both in vitro and in vivo (vs. IR or IR+Veh group), indicating that it deteriorated severely the endothelium IR induced by HG or HFD (Figure 2A-F).

### 3.3 | PPAR $\gamma$ improves endothelium-dependent vasodilation in IR rats

As endothelial dysfunction occurs followed the vascular endothelial IR, we next examined the effects of PPAR $\gamma$  expression on endothelium-dependent vasodilation in vivo. As expected, the endothelium-dependent vasodilation induced by Ach in IR rats (IR group) was decreased by up to 70% compared with the Ctrl rats, whereas the endothelium-independent vasodilation caused by SNP failed to be affected at all in IR rats (IR group). Overexpression of PPAR $\gamma$ , nevertheless, almost restored the endothelium-dependent vasodilation damaged by HFD rather than the endothelium-independent vasodilation (Figure 3A,B); down-expression of PPAR $\gamma$ , in contrast, worsened the endothelium-dependent rather than endothelium-independent vasodilation damaged by HFD (Figure 3C,D).

### 3.4 | Effects of PPAR $\gamma$ levels on eNOS expression in vitro and in vivo

The effects of PPAR $\gamma$  levels on eNOS expression in vitro and in vivo were examined. As predicted, marked decreases of eNOS expression levels were visualized both in the IR HUVEC and the IR rats. Overexpression of PPAR $\gamma$ , nonetheless, strikingly reversed the decreases of eNOS expression levels induced by HG or HFD and down-expression of PPAR $\gamma$  expedited the decreases of eNOS expression levels both in vitro and in vivo (Figure 4A-D).

### 3.5 | Effects of PPAR $\gamma$ on p-IKK $\alpha/\beta$ and I $\kappa$ B $\alpha$ expression in vivo and in vitro

Compared with Ctrl group, the IKK $\alpha/\beta$  level in the IR group was not significantly changed, but the p-IKK $\alpha/\beta$  level was increased by up to 195%. However, overexpression of PPAR $\gamma$  dramatically antagonized the increase of p-IKK $\alpha/\beta$  induced by HG or HFD and down-expression of PPAR $\gamma$  enhanced the increase of the p-IKK $\alpha/\beta$  level induced

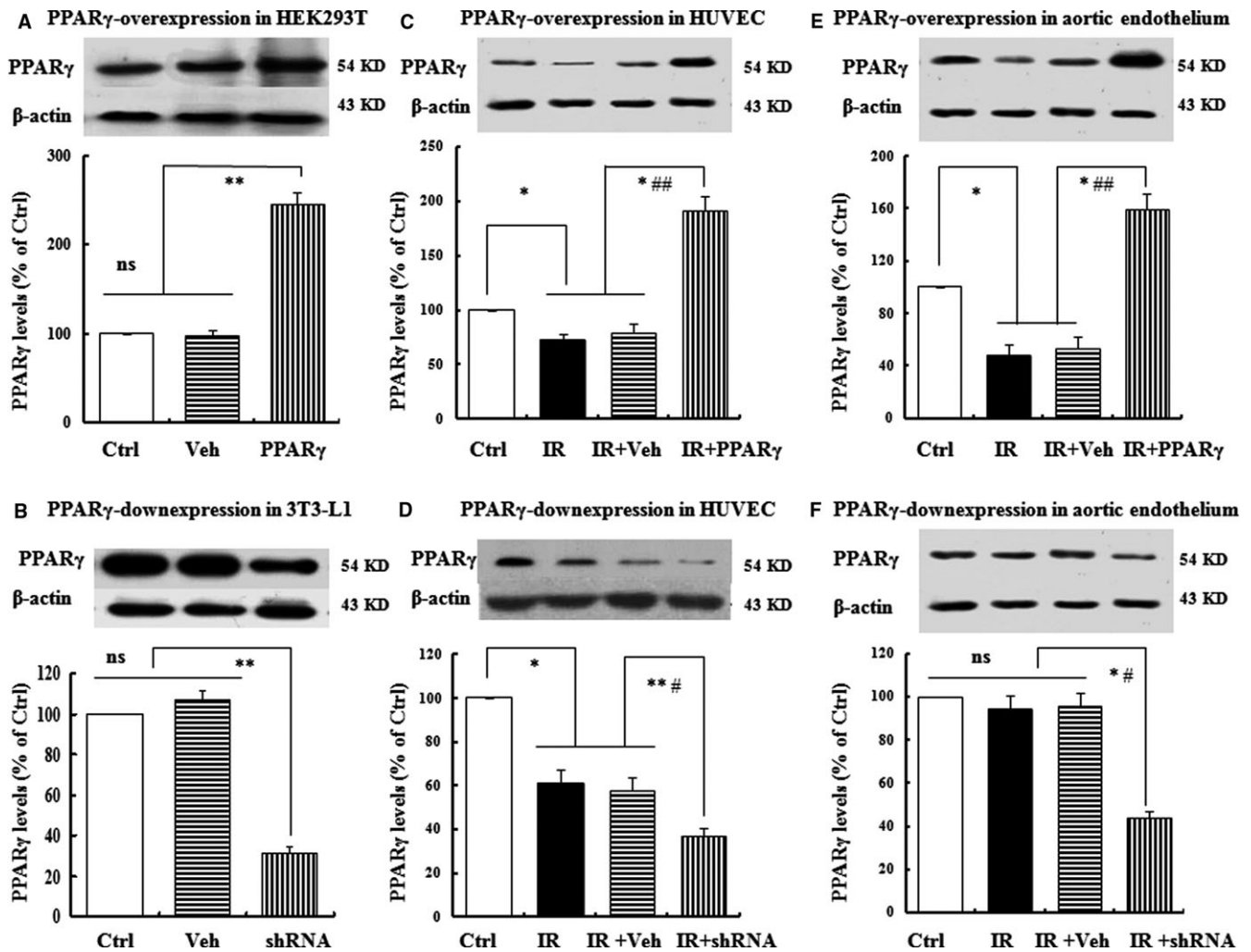


**FIGURE 1** PPAR $\gamma$  expression in HEK293T, 3T3-L1 and vascular endothelial cells in vitro and in vivo. The 90% confluent HEK293T cells (A) and 3T3-L1 cells (B) were transfected with Ad-PPAR $\gamma$  and Ad-PPAR $\gamma$ -shRNA respectively. Besides, the 90% confluent HUVEC were pre-treated with freshly prepared complete DMEM containing HG for 48 h and then transfected with Ad-PPAR $\gamma$  (C), Ad-PPAR $\gamma$ -shRNA (D) and their respective scrambles (Vehicle) respectively. After transfection for 24 h, the cells were washed with PBS twice and further cultured with fresh serum-free DMEM for an additional 12 h. Finally, the cells were harvested and PPAR $\gamma$  expression levels were detected by Western blots. In addition, the aortic endothelia from rats transfected with Ad-PPAR $\gamma$  (E) and Ad-PPAR $\gamma$ -shRNA containing adenoviral vectors (F) were used to examine the PPAR $\gamma$  expression levels by Western blots. Data are expressed as mean  $\pm$  SEM of 4 in vitro and 6 in vivo independent experiments, respectively. \* $P$  < 0.05, \*\* $P$  < 0.01, vs. Ctrl; # $P$  < 0.05, ## $P$  < 0.01, vs. IR or IR+Veh, ns = no significance. Ctrl: normal control, IR: insulin resistance, Veh: vehicle, PPAR $\gamma$ : Ad-PPAR $\gamma$ , shRNA: Ad-PPAR $\gamma$ -shRNA, IR+Veh: IR+vehicle, IR+PPAR $\gamma$ : IR+Ad-PPAR $\gamma$ , IR+shRNA: IR+Ad-PPAR $\gamma$ -shRNA

by HG or HFD both in vitro and in vivo (Figure 5A,B). Besides, compared with the Ctrl group, the I $\kappa$ B $\alpha$  level in the IR group was markedly decreased. Nevertheless, overexpression of PPAR $\gamma$  strikingly counteracted whereas the down-expression expedited the decrease of I $\kappa$ B $\alpha$  level induced by HG or HFD (Figure 5C,D).

### 3.6 | Physical interaction of PPAR $\gamma$ with P65 contributes to decreases of cytokines in HUVEC

As shown in Figure 6A,B, after exposure of HUVEC to HG for 48 hours, both endogenous and exogenous interaction of PPAR $\gamma$  with P65 occurred. Since the interaction of PPAR $\gamma$  with P65 hinders the binding of heterodimer of P65 and p50 to the promoter of

target genes, the levels of cytokines including TNF $\alpha$ , IL-6, sICAM-1 and sVCAM-1 were tested. As anticipated, the levels of TNF $\alpha$ , IL-6, sICAM-1 and sVCAM-1 in IR group were increased by 62%, 50%, 56% and 65% respectively (vs. Ctrl). However, overexpression of PPAR $\gamma$  opposed whereas the down-expression worsened the increases induced by HG (Figure 6C-F).

### 3.7 | Effects of PPAR $\gamma$ expression on the levels of cytokines in the IR rats

The levels of serum cytokines including TNF $\alpha$ , IL-6, sICAM-1 and sVCAM-1 were tested in the IR rats. Consistent with those in vitro, the levels of TNF $\alpha$ , IL-6, sICAM-1 and sVCAM-1 in IR rats were

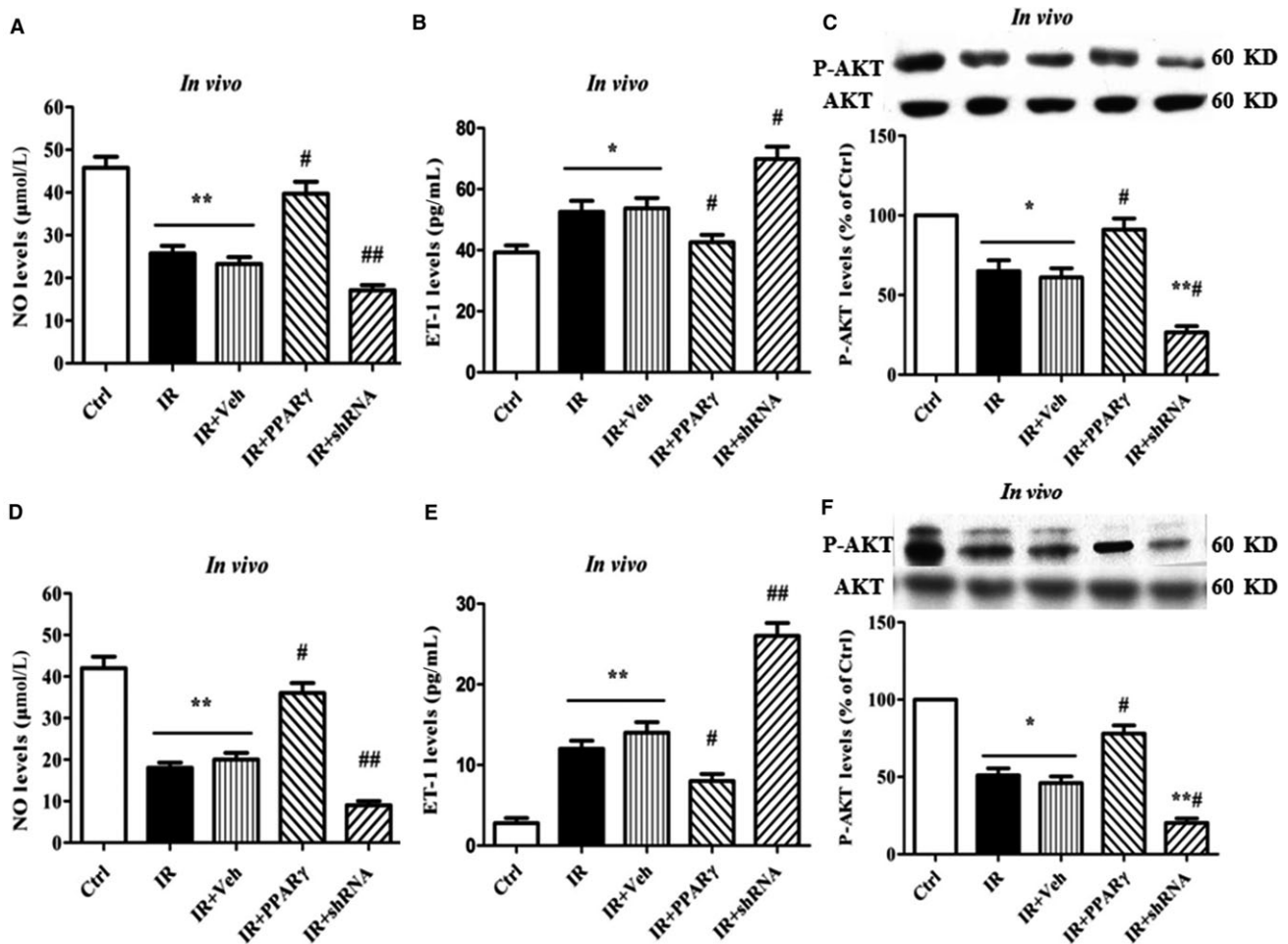


**FIGURE 2** Amelioration of vascular endothelium IR in vitro and in vivo by PPAR $\gamma$ . The 90% confluent HUVEC were pretreated with freshly prepared complete DMEM containing HG for 48 h and then transfected with Ad-PPAR $\gamma$ , Ad-PPAR $\gamma$ -shRNA and their respective scrambles (Vehicle), respectively. After transfection for 24 h, the cells were washed with PBS twice and further cultured with fresh serum-free DMEM for additional 12 h. Subsequently, the cells were treated with insulin ( $5 \text{ mIU L}^{-1}$ , final concentration) for 10 min. At the end, the supernatants were collected and used for the assay of the levels of nitrite (A) and ET-1(B); and the cells were used to detect the expression of AKT and p-AKT (C). Besides, the serum levels of nitrite (D) and ET-1(E) as well as the expression of AKT and p-AKT from aorta tissue (F) in Ad-PPAR $\gamma$ -containing rats and Ad-PPAR $\gamma$ -shRNA-containing rats were measured. Data are expressed as mean  $\pm$  SEM of 4 in vitro and 6 in vivo independent experiments respectively. \* $P < 0.05$ , \*\* $P < 0.01$ , vs. Ctrl; # $P < 0.05$ , ## $P < 0.01$ , vs. IR or IR+Veh. Ctrl: normal control, IR: insulin resistance, IR+Veh: IR+vehicle, IR+PPAR $\gamma$ : IR+Ad-PPAR $\gamma$ , IR+shRNA: IR+Ad-PPAR $\gamma$ -shRNA

increased by 64%, 113%, 230% and 62% respectively (vs. Ctrl group). However, overexpression of PPAR $\gamma$  notably reduced while the down-expression further elevated the increased serum cytokines induced by HFD (Figure 7A-D).

## 4 | DISCUSSION

PPAR $\gamma$  is a nuclear receptor that acts as a transcription factor upon activation, by regulating the transcription and expression of specific genes encoding proteins involved in insulin signalling and gluco-lipid metabolism. PPAR $\gamma$  is highly expressed in adipose tissue, skeletal muscle, liver, pancreatic  $\beta$ -cells, heart, colon, placenta and in the cells of vascular and immune systems<sup>25</sup> and plays critical roles in regulating insulin sensitivity, gluco-lipid metabolism and adipogenesis.<sup>10,26,27</sup>

In the current study, we have shown overexpression of PPAR $\gamma$  notably increased the levels of NO, eNOS, p-AKT, I $\kappa$ B $\alpha$  and the interaction of PPAR $\gamma$  and NF $\kappa$ B-P65, and decreased the levels of ET-1, p-IKK $\alpha$ / $\beta$ , TNF $\alpha$ , IL-6, sICAM-1 and sVCAM-1. In contrast, down-expression of PPAR $\gamma$  showed opposite effects. The findings might suggest PPAR $\gamma$  is a potential therapeutic target for diabetic vascular complications.

In the study, we have shown that PPAR $\gamma$  was highly expressed in 3T3-L1 cells, moderately expressed in HUVEC and HEK293T cells. Therefore, we chose the three cell lines to evaluate the transfection efficacy of viral vectors carrying a full-length cDNA and shRNA targeted PPAR $\gamma$  gene. Both in vitro and in vivo experiments showed that the transfection of viruses carrying a full-length cDNA of PPAR $\gamma$  significantly up-regulated the expression of PPAR $\gamma$ , while the transfection of viruses carrying a shRNA-PPAR $\gamma$  notably down-regulated

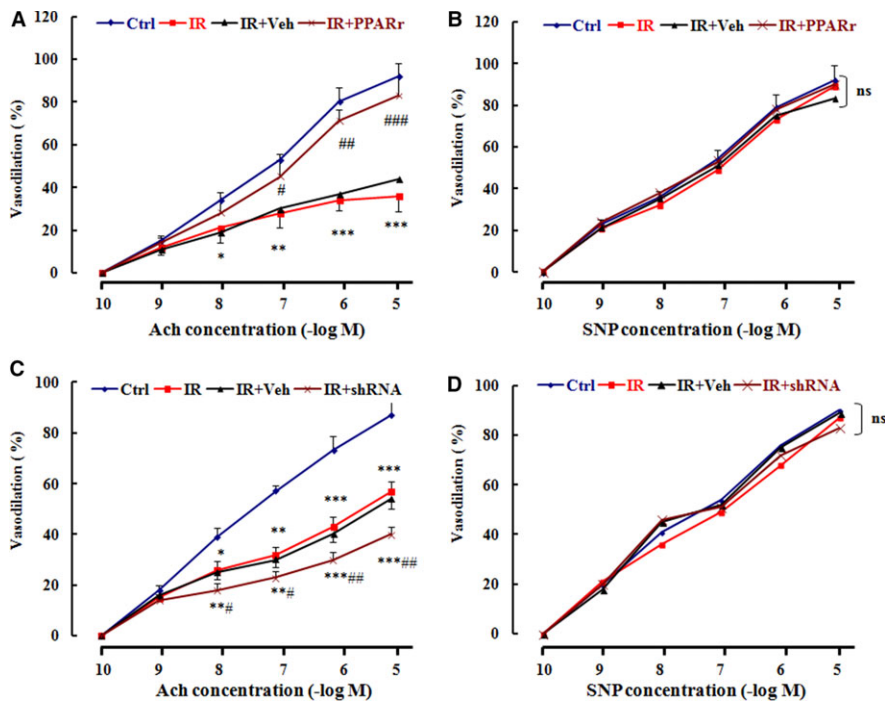


**FIGURE 3** PPAR $\gamma$  improves endothelium-dependent vasodilation in the IR rats. The rats in IR+PPAR $\gamma$  or IR+shRNA group were intravenously administered with Ad-PPAR $\gamma$  or Ad-PPAR $\gamma$ -shRNA respectively, while the rats in IR or IR + Veh group were intravenously given normal saline or a vehicle. The rats that were neither treated with HFD nor transfected were considered as a normal control group (Ctrl). Then, the rat aorta was used to assess the vasodilation function 1 week after treatment. Data are expressed as mean  $\pm$  SEM of 6 rats. \* $P$  < 0.05, \*\* $P$  < 0.01, \*\*\* $P$  < 0.001, vs. Ctrl; # $P$  < 0.05, ## $P$  < 0.01, vs. IR or IR+Veh, ns = no significance. Ach: acetylcholine, SNP: sodium nitroprusside. Ctrl: normal control, IR: insulin resistance, IR+Veh: IR+vehicle, IR+PPAR $\gamma$ : IR+Ad-PPAR $\gamma$ , IR+shRNA: IR+Ad-PPAR $\gamma$ -shRNA

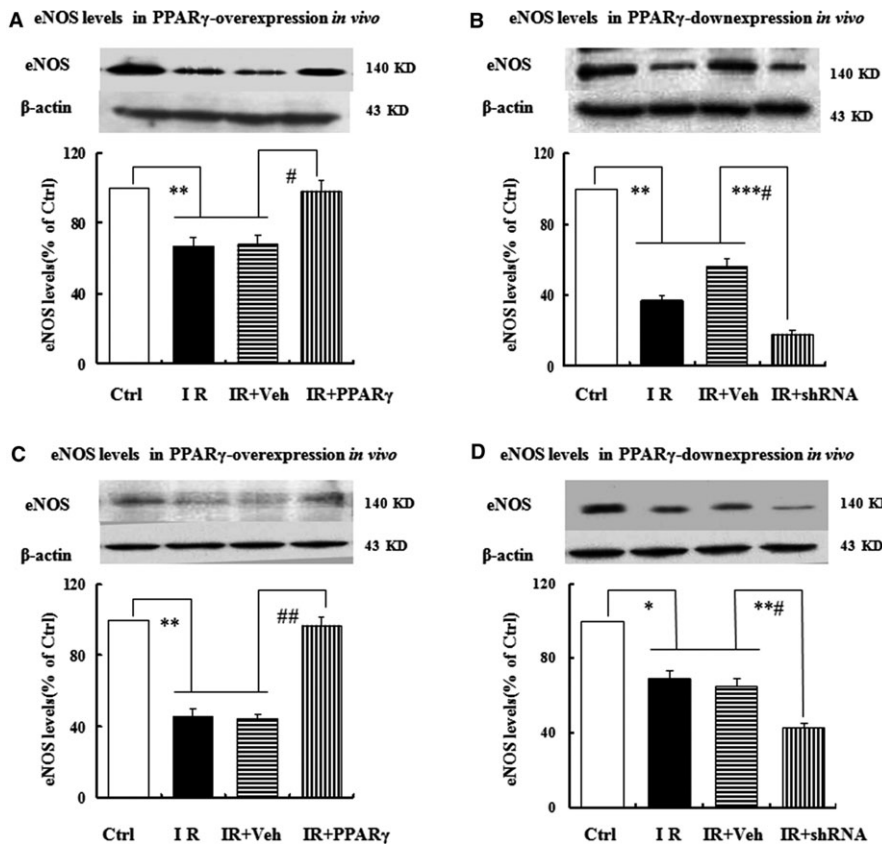


**FIGURE 4** Effects of PPAR $\gamma$  on eNOS expression in vitro and in vivo. The expression levels of eNOS were examined by Western blots when PPAR $\gamma$  were over-expressed in vitro (A) and in vivo (C), and down-expressed in vitro (B) and in vivo (D). The grouping and treatments in vitro and in vivo were the same as described in Figures 2 and 3, and data are expressed as mean  $\pm$  SEM of 4 in vitro and 6 in vivo independent experiments, respectively. \* $P$  < 0.05, \*\* $P$  < 0.01, \*\*\* $P$  < 0.001, vs. Ctrl; # $P$  < 0.05, ## $P$  < 0.01, vs. IR or IR+Veh. Ctrl: normal control, IR: insulin resistance, IR+Veh: IR+vehicle, IR+PPAR $\gamma$ : IR+Ad-PPAR $\gamma$ , IR+shRNA: IR+Ad-PPAR $\gamma$ -shRNA

the expression of PPAR $\gamma$ , indicating that construction and transfection of the viral vectors were successful.

Next we tested whether the changes of PPAR $\gamma$  expression levels affected endothelium IR and dysfunction. It is well known that

vascular endothelium is not only a vascular barrier, but also an important endocrinal organ.<sup>28</sup> It secretes numerous vasoactive substances including NO and ET-1 to fine-tune normal vessel integrity and tension stimulated by a physiological dose of insulin.<sup>29</sup>

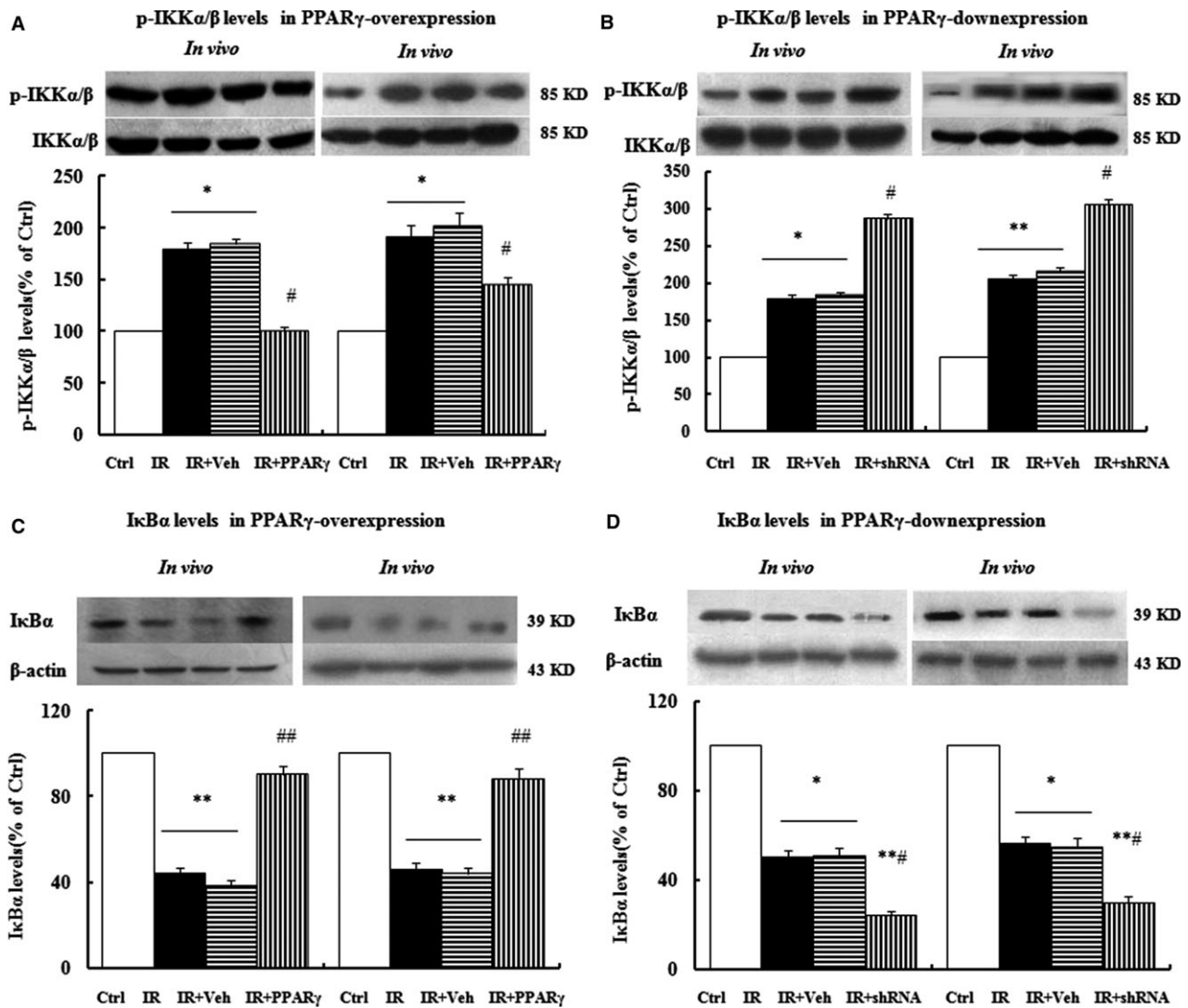


**FIGURE 5** Effects of PPAR $\gamma$  on p-IKK $\alpha/\beta$  and I $\kappa$ B $\alpha$  expression in vitro and in vivo. The expression levels of p-IKK $\alpha/\beta$  and I $\kappa$ B $\alpha$  were examined by Western blots when PPAR $\gamma$  were over-expressed in vitro and in vivo (A, C), and down-expressed in vitro and in vivo (B, D). The grouping and processing in vitro and in vivo were the same as described in Figures 2 and 3, and data are expressed as mean  $\pm$  SEM of 4 in vitro and 6 in vivo independent experiments, respectively. \* $P < 0.05$ , \*\* $P < 0.01$ , vs. Ctrl; # $P < 0.05$ , ## $P < 0.01$ , vs. IR or IR+Veh. Ctrl: normal control, IR: insulin resistance, IR+Veh: IR+vehicle, IR+PPAR $\gamma$ : IR+Ad-PPAR $\gamma$ , IR+shRNA: IR+Ad-PPAR $\gamma$ -shRNA

Production of NO and ET-1 induced by insulin is modulated by IRS-1/PI3K/AKT/NO and Raf/MAPK/ERK/ET-1 pathways. Under normal conditions, the two pathways are kept in a balance. However, due to long-term hyperglycaemia, hyperlipidemia and hyperinsulinemia, the balance is broken and the endothelium IR and dysfunction resultantly occurs, which results in cardio-cerebral vessel event cascades.<sup>30,31</sup> Accordingly, NO and ET-1 are often chosen as the markers of endothelium IR.<sup>24</sup> In the current study, we have demonstrated that exposure of HG or HFD noticeably decreased the NO levels but increased the ET-1 levels, resulting in the endothelium IR, and we further identified that endothelium IR and dysfunction which were induced by HG or HFD were mediated by an NF $\kappa$ B-independent pathway. Over-production of reactive oxygen species (ROS) induced by HG or HFD activated IKK $\alpha/\beta$ , a crucial component of NF $\kappa$ B pathway, and the activated IKK $\alpha/\beta$  interacted physically with

insulin receptor substrate-1 (IRS-1) or Raf and further respectively phosphorylated IRS-1 and Raf. Consequently, the insulin conventional pathway (IRS-1/PI3K/AKT/NO pathway) was blocked, resulting in a weakening of IRS-1/PI3K/AKT/NO pathway and an enhancement of Raf/MAPK/ERK/ET-1 pathway (data not shown). However, overexpression of PPAR $\gamma$  dramatically normalized the changes of NO and ET-1 induced by HG, while down-expression of PPAR $\gamma$  expedited the changes triggered by HG. Similar results were also obtained from in vivo experiments. All of these data suggest that overexpression of PPAR $\gamma$  ameliorates whereas down-expression of PPAR $\gamma$  worsens the endothelium IR.

As vascular endothelium IR and endothelium dysfunction appears successively in the development of AS, it is necessary to distinguish whether the changes of PPAR $\gamma$  expression levels affect endothelial or vascular smooth muscle function in vivo. In general, vasodilation



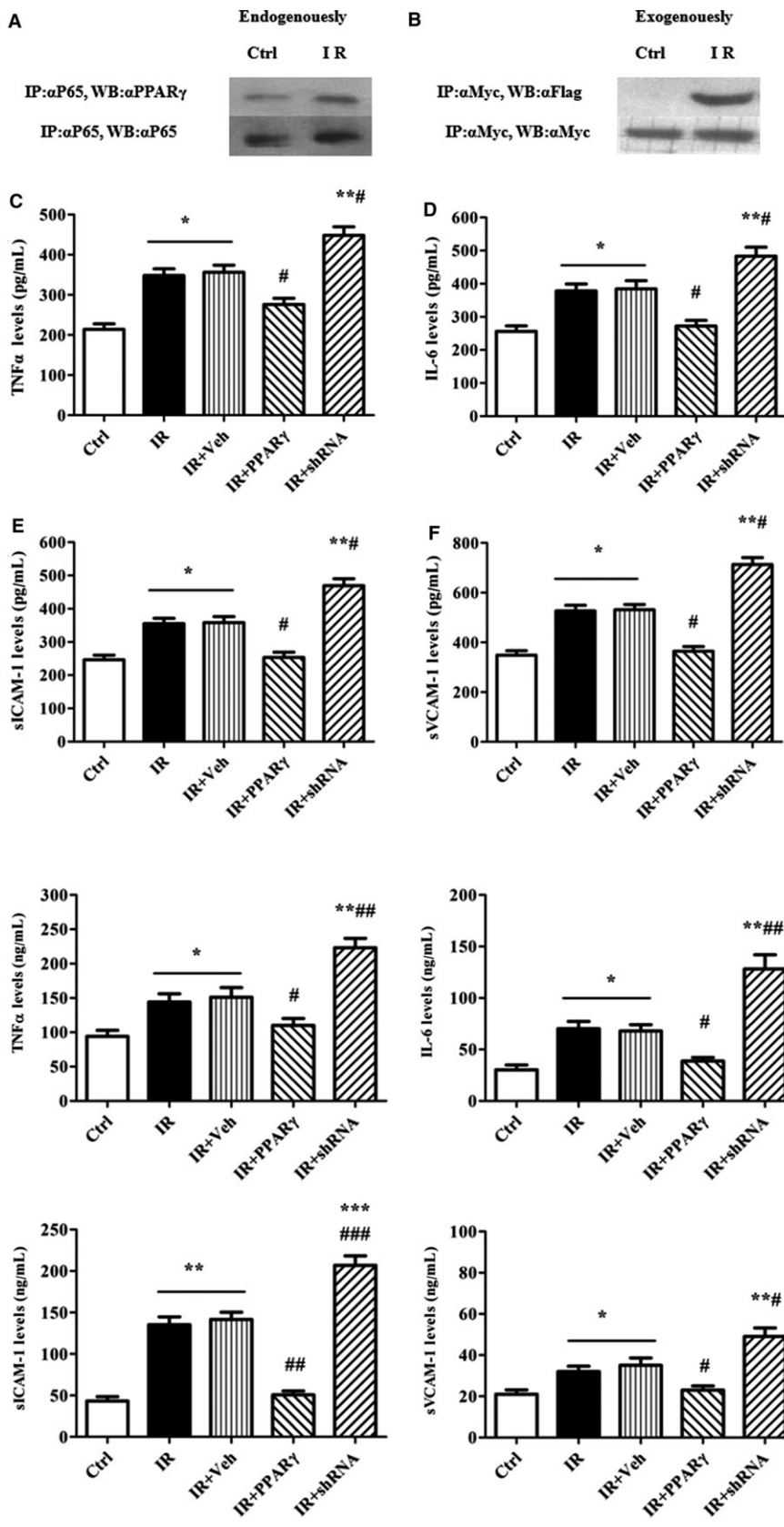


**FIGURE 6** Physical interaction of PPAR $\gamma$  with P65 contributes to decreases of cytokines in HUVEC. The cells were harvested to assay the association of PPAR $\gamma$  with NF $\kappa$ B-P65 by immunoprecipitation (A and B) and the supernatants were used to measure the levels of TNF $\alpha$  (C), IL-6 (D), sICAM-1(E), and sVCAM-1(F) by ELISA. The grouping and processing were the same as described in Figure 2 and data are expressed as mean  $\pm$  SEM of 4 independent experiments. \* $P$  < 0.05, \*\* $P$  < 0.01, vs. Ctrl; # $P$  < 0.05, vs. IR or IR+Veh. Ctrl: normal control, IR: insulin resistance, IR+Veh: IR+vehicle, IR+PPAR $\gamma$ : IR+Ad-PPAR $\gamma$ , IR+shRNA: IR+Ad-PPAR $\gamma$ -shRNA

**FIGURE 7** Effects of PPAR $\gamma$  expression levels on the levels of cytokines in IR rats. The serum levels of TNF $\alpha$  (A), IL-6 (B), sICAM-1(C), and sVCAM-1(D) were measured by ELISA. The grouping and processing were the same as described in Figure 3 and data are expressed as mean  $\pm$  SEM of 6 rats. \* $P$  < 0.05, \*\* $P$  < 0.01, \*\*\* $P$  < 0.001, vs. Ctrl; # $P$  < 0.05, ### $P$  < 0.01, #### $P$  < 0.001, vs. IR or IR+Veh. Ctrl: normal control, IR: insulin resistance, IR+Veh: IR+vehicle, IR+PPAR $\gamma$ : IR+Ad-PPAR $\gamma$ , IR+shRNA: IR+Ad-PPAR $\gamma$ -shRNA

is composed of endothelium-dependent induced by Ach and endothelium-independent triggered by SNP. The former reflects the endothelium function while the latter does vascular smooth muscle

function.<sup>32</sup> Our present data revealed that in the aorta from the IR rat, the endothelium-dependent vasodilation induced by Ach was severely damaged but the endothelium-independent vasodilation

triggered by SNP was not at all, suggesting that in IR or early state of diabetes, dysfunction of endothelial cells occurs while the function of vascular smooth muscle cells remains intact. However, overexpression of PPAR $\gamma$  considerably improved the endothelium-dependent rather than the endothelium-independent vasodilation. In contrast, down-expression of PPAR $\gamma$  significantly exacerbated the endothelium-dependent vasodilation but had no effect on the endothelium-independent vasodilation. Taken together, these data suggest that the changes of PPAR $\gamma$  expression levels indeed influence function of endothelium rather than vascular smooth muscle.

As discussed above, overexpression of PPAR $\gamma$  improves endothelium IR and function, which is involved in the production and availability of NO. It is well known that eNOS catalyzes L-arginine to convert into NO in vascular endothelium under insulin stimulation. NO diffuses into VSMC where it activates guanylate cyclase (GC). Activated GC catalyzes GTP to form GMP which sequentially activates protein kinase G (PKG). PKG ultimately leads to a decrease of free cytoplasm calcium concentration, which further results in dephosphorylation of myosin light chain (MLC) and vasodilation.<sup>33</sup> In the current study, we have shown that HG or HFD reduced the expression levels of eNOS and PPAR $\gamma$ . Nevertheless, overexpression of PPAR $\gamma$  markedly reversed the reduction of eNOS expression levels induced by HG or HFD; conversely, down-expression of PPAR $\gamma$  significantly deteriorated the reduction, suggesting that eNOS-dependent NO production is mediated by PPAR $\gamma$ .

Various studies have confirmed that IR and AS are a chronic inflammation process.<sup>34,35</sup> Besides regulating the metabolism of gluco-lipids and adipogenesis, PPAR $\gamma$  has an anti-inflammatory effect.<sup>36,37</sup> A large number of studies have reported that PPAR $\gamma$  plays above-mentioned roles mainly via two mechanisms.<sup>38-40</sup> One is the trans-activation of PPAR $\gamma$ -dependent insulin pathway, and the other is the trans-repression of PPAR $\gamma$ -dependent NF $\kappa$ B pathway. The former is a canonical mechanism; that is, upon activation by endogenous or synthetic ligands, PPAR $\gamma$  heterodimerizes with retinoid X receptor (RXR). The PPAR $\gamma$ /RXR heterodimer undergoes conformational changes which alter co-activator/co-repressor dynamics and binds further to PPRE in the promoter region of the target genes. Thus, transcription initiation of the target genes takes place.<sup>41,42</sup> The latter is a non-canonical mechanism; namely, activated PPAR $\gamma$ /RXR heterodimer interacts physically with NF $\kappa$ B and impedes NF $\kappa$ B to bind with the promoter region of the target genes encoding inflammation factors such as TNF $\alpha$ , IL-6, sICAM-1 and sVCAM-1 and therefore plays anti-inflammation.<sup>43,44</sup>

However, it is unclear whether the changes of PPAR $\gamma$  expression affect NF $\kappa$ B pathway. In the study, we have shown that HG or HFD indeed increased the levels of p-IKK $\alpha$ / $\beta$  and cytokines including TNF $\alpha$ , IL-6, sICAM-1 and sVCAM-1 and decreased the I $\kappa$ B $\alpha$  levels. It might be due to the fact that activated IKK $\alpha$ / $\beta$ , an upstream kinase of I $\kappa$ B $\alpha$ , phosphorylates I $\kappa$ B $\alpha$  at the sites of serine 32 and 36, leads to the I $\kappa$ B $\alpha$  degradation, and then gives rise to the translocation and activation of NF $\kappa$ B (P65/P50), and eventually causes the expression of inflammation genes (TNF $\alpha$ , IL-6, sICAM-1 and sVCAM-1, etc). Nonetheless, overexpression of PPAR $\gamma$  markedly normalized the changes induced by HG or HFD and promoted the interaction

between PPAR $\gamma$  and NF $\kappa$ B-P65. By contrary, down-expression of PPAR $\gamma$  significantly enhanced the changes induced by HG or HFD. These data demonstrate that overexpression of PPAR $\gamma$  may repress NF $\kappa$ B trans-activation and improve the endothelium IR through a PPAR $\gamma$ -dependent NF $\kappa$ B trans-repression mechanism.

In conclusion, the present study confirmed that the changes of PPAR $\gamma$  expression affected endothelium IR. Overexpression of PPAR $\gamma$  improved endothelium IR while down-expression of PPAR $\gamma$  worsened endothelium IR via a PPAR $\gamma$ -dependent NF $\kappa$ B trans-repression pathway. Since loss of PPAR $\gamma$  function exists in the patients with T2DM and AS,<sup>45</sup> the current findings suggest PPAR $\gamma$  is a potential therapeutic target for diabetic vascular complications.

## ACKNOWLEDGEMENTS

This study was supported by the research grants from the National Natural Scientific Foundation of China (81070633, 81360060, 31660323 and 30860111) and the research project from the Jiangxi Provincial Department of Science and Technology (20123BCB22005).

## CONFLICT OF INTEREST

The authors confirm that there are no conflicts of interest.

## AUTHOR CONTRIBUTIONS

Y. Kong, Y. Gao, D. Lan and Y. Zhang performed the research. Q. Huang and Y. Kong designed the research. Q. Huang, R. Zhan, M. Liu, Z. Zhu, and G. Zeng analysed the data. Q. Huang and Y. Kong wrote the paper. D. Lan, Y. Zhang, R. Zhan, M. Liu, Z. Zhu, and G. Zeng reviewed and edited the paper.

## ORCID

Qiren Huang  <http://orcid.org/0000-0002-3434-9484>

## REFERENCES

- Toral M, Gomez-Guzman M, Jimenez R, et al. Chronic peroxisome proliferator-activated receptorbeta/delta agonist GW0742 prevents hypertension, vascular inflammatory and oxidative status, and endothelial dysfunction in diet-induced obesity. *J Hypertens*. 2015;33:1831-1844.
- Li Kwok Cheong JD, Croft KD, Henry PD, et al. Green coffee polyphenols do not attenuate features of the metabolic syndrome and improve endothelial function in mice fed a high fat diet. *Arch Biochem Biophys*. 2014;559:46-52.
- Donato AJ, Henson GD, Hart CR, et al. The impact of ageing on adipose structure, function and vasculature in the B6D2F1 mouse: evidence of significant multisystem dysfunction. *J Physiol*. 2014;592:4083-4096.
- Park Y, Booth FW, Lee S, et al. Physical activity opposes coronary vascular dysfunction induced during high fat feeding in mice. *J Physiol*. 2012;590:4255-4268.
- Alberti KG, Zimmet P, Shaw J, et al. The metabolic syndrome—a new worldwide definition. *Lancet*. 2005;366:1059-1062.

6. Despres JP, Lemieux I. Abdominal obesity and metabolic syndrome. *Nature*. 2006;444:881-887.
7. Manrique C, Lastra G, Sowers JR. New insights into insulin action and resistance in the vasculature. *Ann N Y Acad Sci*. 2014;1311:138-150.
8. Vinet A, Obert P, Dutheil F, et al. Impact of a lifestyle program on vascular insulin resistance in metabolic syndrome subjects: the RESOLVE study. *J Clin Endocrinol Metab*. 2015;100:442-450.
9. Drouin-Chartier JP, Brassard D, Tessier-Grenier M, et al. Systematic review of the association between dairy product consumption and risk of cardiovascular-related clinical outcomes. *Adv Nutr*. 2016;7:1026-1040.
10. Ang S, Dougherty EJ, Danner RL. PPAR $\gamma$  signaling and emerging opportunities for improved therapeutics. *Pharmacol Res*. 2016;111:76-85.
11. Colca JR. The TZD insulin sensitizer clue provides a new route into diabetes drug discovery. *Expert Opin Drug Discov*. 2015;10:1259-1270.
12. Nathan DM. Diabetes: advances in diagnosis and treatment. *JAMA*. 2015;314:1052-1062.
13. Joshi SR. Saroglitazar for the treatment of dyslipidemia in diabetic patients. *Expert Opin Pharmacother*. 2015;16:597-606.
14. Fonseca VA. Rationale for the use of insulin sensitizers to prevent cardiovascular events in type 2 diabetes mellitus. *Am J Med*. 2007;120:S18-S25.
15. Yoshimoto T, Naruse M, Shizume H, et al. Vasculo-protective effects of insulin sensitizing agent pioglitazone in neointimal thickening and hypertensive vascular hypertrophy. *Atherosclerosis*. 1999;145:333-340.
16. Ferrannini E, DeFronzo RA. Impact of glucose-lowering drugs on cardiovascular disease in type 2 diabetes. *Eur Heart J*. 2015;36:2288-2296.
17. Goltsman I, Khoury EE, Winaver J, et al. Does Thiazolidinedione therapy exacerbate fluid retention in congestive heart failure? *Pharmacol Ther*. 2016;168:75-97.
18. Lee BC, Lee J. Cellular and molecular players in adipose tissue inflammation in the development of obesity-induced insulin resistance. *Biochim Biophys Acta*. 2014;1842:446-462.
19. Zhang Y, Zhan RX, Chen JQ, et al. Pharmacological activation of PPAR gamma ameliorates vascular endothelial insulin resistance via a non-canonical PPARgamma- dependent nuclear factor-kappa B trans-repression pathway. *Eur J Pharmacol*. 2015;754:41-51.
20. Huang QR, Li Q, Chen YH, et al. Involvement of anion exchanger-2 in apoptosis of endothelial cells induced by high glucose through an mPTP-ROS-Caspase-3 dependent pathway. *Apoptosis*. 2010;15:693-704.
21. Zhong XJ, Shen XD, Wen JB, et al. Osteopontin-induced brown adipogenesis from white preadipocytes through a PI3K-AKT dependent signaling. *Biochem Biophys Res Commun*. 2015;459:553-559.
22. Liu LL, Yan L, Chen YH, et al. A role for diallyl trisulfide in mitochondrial antioxidative stress contributes to its protective effects against vascular endothelial impairment. *Eur J Pharmacol*. 2014;725:23-31.
23. Liu D, Wu M, Lu Y, et al. Protective effects of 6-Gingerol on vascular endothelial cell injury induced by high glucose via activation of PI3K-AKT-eNOS pathway in human umbilical vein endothelial cells. *Biomed Pharmacother*. 2017;93:788-795.
24. Kearney MT, Duncan ER, Kahn M, et al. Insulin resistance and endothelial cell dysfunction: studies in mammalian models. *Exp Physiol*. 2008;93:158-163.
25. Thangavel N, Al Bratty M, Akhtar Javed S, et al. Targeting peroxisome proliferator-activated receptors using thiazolidinediones: strategy for design of novel antidiabetic drugs. *Int J Med Chem*. 2017;2017:1069718.
26. Chen Y, Ma H, Zhu D, et al. Discovery of novel insulin sensitizers: promising approaches and targets. *PPAR Res*. 2017;2017:8360919.
27. Alemán-González-Duhart D, Tamay-Cach F, Álvarez-Almazán S, et al. Current advances in the biochemical and physiological aspects of the treatment of type 2 diabetes mellitus with thiazolidinediones. *PPAR Res*. 2016;2016:7614270.
28. Jensen HA, Mehta JL. Endothelial cell dysfunction as a novel therapeutic target in atherosclerosis. *Expert Rev Cardiovasc Ther*. 2016;14:1021-1033.
29. Baratchi S, Khoshmanesh K, Woodman OL, et al. Molecular sensors of blood flow in endothelial cells. *Trends Mol Med*. 2017;23:850-868.
30. Potenza MA, Marasciulo FL, Chieppa DM, et al. Insulin resistance in spontaneously hypertensive rats is associated with endothelial dysfunction characterized by imbalance between NO and ET-1 production. *Am J Physiol*. 2005;289:H813-H822.
31. Hitomi H, Kaifu K, Fujita Y, et al. Angiotensin II shifts insulin signaling into vascular remodeling from glucose metabolism in vascular smooth muscle cells. *Am J Hypertens*. 2011;24:1149-1155.
32. Mordi I, Mordi N, Delles C, et al. Endothelial dysfunction in human essential hypertension. *J Hypertens*. 2016;34:1464-1472.
33. Vanhoutte PM, Zhao Y, Xu A, et al. Thirty years of saying NO: sources, fate, actions, and misfortunes of the endothelium-derived vasodilator mediator. *Circ Res*. 2016;119:375-396.
34. Matsuda M, Shimomura I. Roles of oxidative stress, adiponectin, and nuclear hormone receptors in obesity-associated insulin resistance and cardiovascular risk. *Horm Mol Biol Clin Invest*. 2014;19:75-88.
35. Alexopoulos N, Katritsis D, Raggi P. Visceral adipose tissue as a source of inflammation and promoter of atherosclerosis. *Atherosclerosis*. 2014;233:104-112.
36. Choi S, Jung JE, Yang YR, et al. Novel phosphorylation of PPAR $\gamma$  ameliorates obesity-induced adipose tissue inflammation and improves insulin sensitivity. *Cell Signal*. 2015;27:2488-2495.
37. Kim TK, Park KS. Inhibitory effects of harpagoside on TNF $\alpha$ -induced pro-inflammatory adipokine expression through PPAR- $\gamma$  activation in 3T3-L1 adipocytes. *Cytokine*. 2015;76:368-374.
38. Singh VP, Gurunathan C, Singh S, et al. Genetic deletion of Wdr13 improves the metabolic phenotype of Lepr (db/db) mice by modulating AP1 and PPAR $\gamma$  target genes. *Diabetologia*. 2015;58:384-392.
39. Banks AS, McAllister FE, Camporez JP, et al. An ERK/Cdk5 axis controls the diabetogenic actions of PPAR $\gamma$ . *Nature*. 2015;517:391-395.
40. Liepinsh E, Makrecka-Kuka M, Makarova E, et al. Decreased acylcarnitine content improves insulin sensitivity in experimental mice models of insulin resistance. *Pharmacol Res*. 2016;113:788-795.
41. Silva JC, César FA, de Oliveira EM, et al. New PPAR $\gamma$  partial agonist improves obesity-induced metabolic alterations and atherosclerosis in LDLr(-/-) mice. *Pharmacol Res*. 2016;104:49-60.
42. Xie X, Zhou X, Chen W, et al. L312, a novel PPAR $\gamma$ ligand with potent anti-diabetic activity by selective regulation. *Biochim Biophys Acta*. 2015;1850:62-72.
43. Zhang YF, Zou XL, Wu J, et al. Rosiglitazone, a peroxisome proliferator-activated receptor (PPAR)- $\gamma$  Agonist, attenuates inflammation via NF- $\kappa$ B inhibition in lipopolysaccharide-induced peritonitis. *Inflammation*. 2015;38:2105-2115.
44. Ying W, Tseng A, Chang RC, et al. MicroRNA-223 is a crucial mediator of PPAR $\gamma$ -regulated alternative macrophage activation. *J Clin Invest*. 2015;125:4149-4159.
45. Mukohda M, Stump M, Ketsawatsomkron P, et al. Endothelial PPAR- $\gamma$  provides vascular protection from IL-1 $\beta$ -induced oxidative stress. *Am J Physiol Heart Circ Physiol*. 2016;310:H39-H48.

**How to cite this article:** Kong Y, Gao Y, Lan D, et al. Trans-repression of NF $\kappa$ B pathway mediated by PPAR $\gamma$  improves vascular endothelium insulin resistance. *J Cell Mol Med*. 2019;23:216–226. <https://doi.org/10.1111/jcmm.13913>